Supplemental Material to "Heating-Induced Long-Range η-Pairing in the Hubbard Model"

J. Tindall,[1] B. Buča,[1] J. Coulthard,[1] and D. Jaksch[1,2]

[1]*Clarendon Laboratory, University of Oxford, Parks Road, Oxford OX1 3PU, United Kingdom*

[2]*Centre for Quantum Technologies, National University of Singapore, 3 Science Drive 2, Singapore 117543*

(Dated: June 21, 2019)

NUMERICAL PROCEDURE

The master equation we solve in the main text reads

$$\frac{\partial \rho}{\partial t} = \mathcal{L}\rho = -i[H,\rho] + \gamma \sum_{j=1}^{M} (L_j \rho L_j^\dagger - \frac{1}{2}\{L_j^\dagger L_j, \rho\}), \quad L_j = s_j^z = n_{\uparrow,j} - n_{\downarrow,j}, \tag{1}$$

with

$$H = -\tau \sum_{\langle ij\rangle,\sigma} (c_{\sigma,i}^\dagger c_{\sigma,j} + \text{h.c}) + U \sum_{i=1}^{M} n_{\uparrow,i} n_{\downarrow,i}. \tag{2}$$

For our numerical simulations we perform a stochastic unravelling of this master equation, known as the 'quantum trajectories' approach [1]. We use DMRG (Density Matrix Renormalisation Group) [2] to find the ground state of the Hamiltonian and then evolve this in time using the TEBD (Time Evolving Block Decimation) [3] algorithm. We focus on 1D lattice realisations of the model due to their numerical tractibility. We implemented these algorithms using the TNT (Tensor Network Theory) Library [4]. For all figures within the main text we use a bond-dimension of $\chi = 1000$ to ensure the corresponding SVD (Singular Value Decomposition) errors are minimal and the sum of the squares of the discarded singular values in a given time-step does not exceed $\epsilon = 1 \times 10^{-4}$. Increasing the bond dimension has no effect on our results. For all simulations with a finite value of γ we perform $N = 2000$ trajectories to ensure convergence of the measured observables to within an uncertainty of 2%. We also checked that lowering the timestep δt from the value ($\delta t = 0.01/\tau$) used in our second-order Trotter decomposition of the propagator has no noticeable effect on our results.

Despite using a TEBD approach we are not able to reach particularly large system sizes as the states reached in the long-time limit have both completely long-range entanglement and a significant amount of classical correlations. This can cause the Matrix Product State representation to be highly inefficient [5] and we find the bond dimensions required for our simulations, at least at the levels of the individual trajectories, is large and prevents us from being able to make effective use of the aforementioned Matrix Product algorithms.

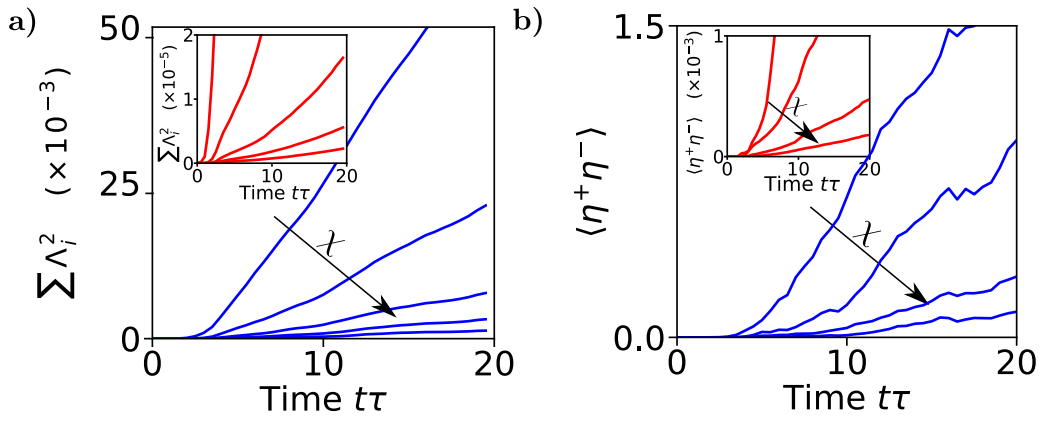

FIG. 1. Simulation starting from the ground state of the $U = \tau$ Hubbard model for $L = 10$ and symmetric half-filling $\left(\langle N_\uparrow\rangle = \langle N_\downarrow\rangle = L/2\right)$. The system is then time-evolved, with the TEBD algorithm, under the Master Equation in Eq. (1) but with $U = 2.0\tau$. The bond dimensions used are $\chi = 100, 200, ..., 500$ with larger χ corresponding to the curves closer to the x-axis. (a) Cumulative total of the squares of the discarded singular values in the TEBD algorithm, averaged over 10 trajectories, for the open system with $\gamma = 2.0\tau$. Inset) Cumulative total of the squares of the discarded singular values in the TEBD algorithm for the closed system ($\gamma = 0.0$). (b) Value of $\langle\eta^+\eta^-\rangle$ during the simulation (which should, for each trajectory, be conserved) for the open system with $\gamma = 2.0\tau$. Inset) Value of, trajectory-averaged, $\langle\eta^+\eta^-\rangle$ during the simulation for the closed system ($\gamma = 0.0$).

In Fig. 1 we demonstrate this: the cumulative total of the squares of the discarded singular values (a measure of the accuracy of the simulation) over time for an average trajectory in the open system is several orders of magnitude larger than that of the corresponding closed system. Unless a very large bond dimension is used this results in a critical failure of the numerics to conserve physical symmetries of the system, such as $\langle\eta^+\eta^-\rangle$ - which should, for each trajectory, always remain 0 in the example considered.

USING SYMMETRY BASED DEPHASING TO INDUCE DISTANCE INVARIANT OFF-DIAGONAL CORRELATIONS

The result of engineering off-diagonal long-range correlations through dissipation is not specific to the Hubbard model nor the choice of Lindblad operators, it is a consequence of the multiple SU(2) symmetries of the Hamiltonian. To illuminate this we define a general Liouvillian map Λ in the manner of (1), with a Hamiltonian H and set of jump operators $\{L_k\}$. We consider the situation when H has at least 2 SU(2) symmetries, i.e. there exists $N \geq 2$ sets of operators $\{J_i^{\pm,z}\}$ $i = 1, 2, ..., N$ where $J_i^{\pm,z}$ are the 3

generators for the SU(2) symmetry i of the Hamiltonian

$$[H, J_i^z] = 0, \quad [H, J_i^\pm] = \pm\mu_i J_i^\pm, \quad [H, J_i^+ J_i^-] = 0,$$
$$[J_i^z, J_{i'}^\pm] = \pm\delta_{i,i'} J_i^\pm, \quad [J_i^+, J_{i'}^-] = 2\delta_{i,i'} J_i^z, \quad \mu_i \in \mathbb{R}. \tag{3}$$

The commutativity between any pairs of generators from two different symmetries is encoded by the Kronecker delta. Any of the operators can be written as a sum of their projectors, via an eigendecomposition, $J_i^{+-,z} = \sum_{\alpha=1}^{D_i^{+-,z}} \lambda_{i,\alpha}^{+-,z} \mathcal{P}_{i,\alpha}^{+-,z}$. We have combined $J_i^\pm$ to form $J_i^{+-} = J_i^+ J_i^-$ due to their mutual eigenspaces.

We now induce dephasing on the model in a symmetry protected manner by choosing $\{L_k\}$ such that

$$[L_k, J_j^{+-,z}] = 0, \tag{4}$$

for at least one symmetry j within $i = 1, 2, ..., N$. Provided that the map is unital ($\sum_k [L_k, L_k^\dagger] = 0$) then the commutation relations in Eq. (3) result in any projector associated with a generator satisfying (4) being a null eigenvector of the Liouvillian map $\Lambda(\mathcal{P}_{j,\alpha}^{+-,z}) = 0$ [6]. The projectors $\mathcal{P}_{j,\alpha}^{+-,z}$ for all the j satisfying (4), and those for the operators $\{C\}$ relating to any remaining conserved quantities [7], fully span the kernel of Λ. It then follows that linear combinations (or any trace-normalised function which can be expanded as a power series) of these projectors is a steady state of the map Λ [6].

Let us write the steady states in this form

$$\rho_{ss} \propto \sum_\beta \lambda_\beta \mathcal{P}_\beta, \tag{5}$$

where the sum is over all the projectors spanning the kernel of Λ. The following analysis is also valid if we write the steady state as any power-series expandable function of these projectors. Assuming we have a lattice model we define a permutation operator $P_{i,i'}$ ($P_{i,i'}^2 = 1$) which exchanges sites i and i'. If all the operators, $\{O\} = \{J_j^{+-,z}\} \bigcup \{C\}$, whose projectors are involved in Eq. (5) are invariant under the same $P_{i,i'}$ then

$$P_{i,i'} O P_{i,i'} = O \implies [O, P_{i,i'}] = 0 \implies [\mathcal{P}_\beta, P_{i,i'}] = 0 \quad \forall\beta. \tag{6}$$

It immediately follows that

$$[\rho_{ss}, P_{i,i'}] = 0. \tag{7}$$

Now let us choose one of the symmetries satisfying (4) and index it by k. The 3 generators for this symmetry are $J_k^{+,-,z}$ and all of their projectors are contained in Eq. (5). We assume they can be written as a sum of

purely local operators on the M site lattice: $J_k^{+,-,z} = \sum_{l=1}^{M} J_{k,l}^{+,-,z}$. Then we define the off-diagonal expectation value

$$\langle J_{k,l}^{+} J_{k,m}^{-} \rangle = \mathrm{Tr}(\rho_{ss} J_{k,l}^{+} J_{k,m}^{-}) \quad l \neq m. \tag{8}$$

We now prove this is invariant under the choice of l and m by using the resolution of identity with the permutation operator $P_{j,j'}$ as well as (7)

$$\begin{aligned} \mathrm{Tr}(\rho_{ss} J_{k,l}^{+} J_{k,m}^{-}) = \mathrm{Tr}(\rho_{ss} P_{l,l'}^2 J_{k,l}^{+} P_{m,m'}^2 J_{k,m}^{-}) = \mathrm{Tr}(\rho_{ss} P_{l,l'} J_{k,l}^{+} P_{l,l'} P_{m,m'} J_{k,m}^{-} P_{m,m'}) \\ = \mathrm{Tr}(\rho_{ss} J_{k,l'}^{+} J_{k,m'}^{-}) \quad l \neq m,\ l' \neq m',\ l \neq m',\ l' \neq m. \end{aligned} \tag{9}$$

We can easily choose the correct combination of indices on the permutation operators to lift the restrictions $l \neq m'$ and $l' \neq m$ and so we get:

$$\langle J_{k,l}^{+} J_{k,m}^{-} \rangle = \langle J_{k,l'}^{+} J_{k,m'}^{-} \rangle \quad l \neq m,\ l' \neq m'. \tag{10}$$

Hence, we show that these correlations have no identifiable length scale as they are uniform for any of the symmetries j, which satisfy (4), if we can find a valid two-site permutation operator which commutes with all the operators $\{O\} = \{J_j^{+-,z}\} \bigcup \{C\}$ at the same time.

In the main text we choose spin dephasing $L_k = s_k^z$ to observe uniform, off-diagonal correlations in the η SU(2) symmetry of the Hubbard model. This dephasing means the η generators satisfy (4) but also that S^z is an additional conserved quantity. Hence $\{O\} = \{\eta^+, \eta^-, \eta^z, S^z\}$, and the kernel of Λ is made up of the projectors of these operators (which are equivalent to the projectors of $\eta^+\eta^-$, $N_\uparrow$, $N_\downarrow$). We can find a valid permutation operator for all of these operators simultaneously - it must swap two sites and carry over a change of sign on the local operators when it does this. We consider initial states (e.g. ground states of the Hamiltonian) which typically have decaying short-range correlations in η pairs. As $\langle \eta^+\eta^- \rangle$ is conserved these correlations will be spread over all length-scales of the system in order to satisfy Eq. (10). Hence, in our simulations, we see uniform off-diagonal correlations in the η sector.

STABILITY OF THE MASTER EQUATION UNDER PERTURBATION

We consider how the dynamics of our model is affected by perturbations in the dephasing. To simulate this we choose additional, 'unwanted', dephasing in the number basis of the system - as well as having $\{L_j\} = s_j^z$ with constant rate $\gamma^s \ \ \forall j$ (see Eq. (1)) we add in another set of local jump operators $\{L_m\} = n_{m,\uparrow} + n_{m,\downarrow}$ with constant rate $\gamma^c = \lambda\gamma^s \ \ \forall m$. The indices j and m each run over the lattice sites in the system. We have used local number dephasing because this additional dephasing breaks the strong

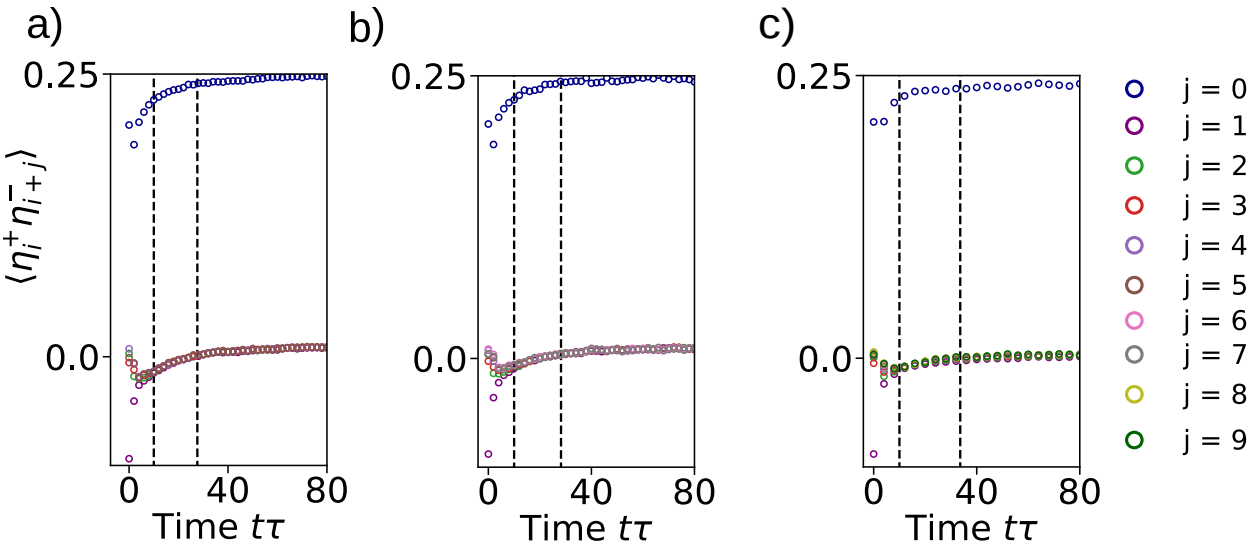

FIG. 2. (top) Dynamics of the, distance-averaged, quantity $\langle \eta_i^+ \eta_{i+j}^- \rangle$ for a quench from the ground state of the $U = \tau$ Hubbard model at half-filling. During the quench dephasing is switched on with jump operators s_i^z and $n_{i,\uparrow} + n_{i,\downarrow}$ on each site i at rates $\gamma^s = 2.0\tau$ and $\gamma^c = 0.02\tau$ respectively. Dashed vertical lines are at $t\tau = 8.0$ and the time when the correlations have decayed to a $1/3$ of their value compared to those at $t\tau = 8.0$. (a) $L = 6$. (b) $L = 8$. (c) $L = 10$.

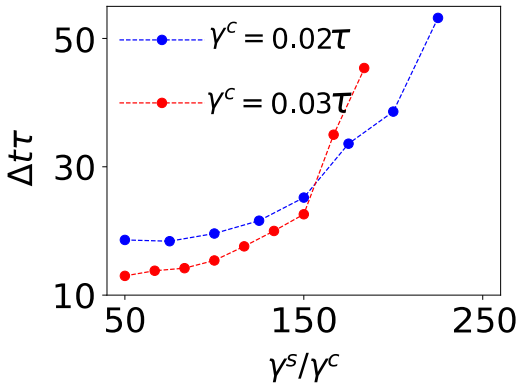

FIG. 3. Time $\Delta t\tau$ for η-correlations to decay to $1/3$ of their value at $t\tau = 8.0$ as a function of the ratio of the spin-dephasing to the charge dephasing for a quench starting from the ground state of the $L = 6$, $U = \tau$ Hubbard model. During the quench dephasing is applied with the values of of γ_c and γ_s specified in the plot.

symmetry relation $[\eta^+\eta^-, L_m] \neq 0 \; \forall m$. Consequently, in the long-time limit this additional dephasing completely destroys any coherences in the system and the steady state is a featureless infinite temperature ensemble.

We set the amplitude of the unwanted dephasing to be around 2 orders of magnitude less than the spin-dephasing. In cold atomic systems parameters can be tuned widely and unwanted decoherence mechanisms strongly suppressed [8]. In quantum materials microscopic models are not as well established. However,

the rates of different decoherence mechanisms can vary widely and careful engineering of these materials can significantly reduce their sensitivity to specific sources of decoherence [9]. As a result decoherence rates can easily differ by orders of magnitude, in line with the assumptions in our work.

Figure 2 shows that, for $\lambda = \gamma^c/\gamma^s = 0.01$, the additional dephasing does not prevent the observation of the ODLRO which forms and is maintained prior to the system decaying to a thermal classical ensemble. The window, indicated by the dashed lines, shows the time it takes for the off-diagonal correlations to decay to $1/3$ of their value at the first dashed line. The data in Fig. 2 suggests the size of this window is not diminishing with system size. This is consistent with previous research studying the rate of relaxation in bulk-dephased many-body systems [10] or in random Liouvillians [11] - they find this rate either decays or saturates with system size.

Additionally, Fig. 3 shows that for small perturbations this window can be lengthened by increasing the ratio γ^s/γ^c. Thus, in an experimental setup, being able to tune γ_s could help mitigate the effects of the unwanted dephasing. Physically, the increased amplitude of the wanted (spin) dephasing compared to the unwanted (number) dephasing means the system is 'measured with increasing frequency by the spin dephasing in comparison to the frequency with which it is 'measured' by the number dephasing. As the ratio of these amplitudes increases then the spin dephasing effectively arrests the time evolution induced by the number-dephasing. Repeated measurements in the spin basis are freezing the systems dynamics with respect to the dissipative evolution caused by the unwanted dephasing.

FLOQUET HEATING

In the main text we discussed that the properties of the steady states of (1) are reproduced by Floquet heating of the spin sector of the Hubbard model to infinite temperature. In order to show this we consider the Hubbard Hamiltonian with an additional time-dependent inhomogeneous magnetic field

$$H(t) = H_{\mathrm{Hubbard}}(U,\tau) + B(t)\sum_{i=1}^{L} f(i)s_i^z, \quad B(t) = V\cos(\Omega t), \tag{11}$$

and $f(i)$ describes the inhomogeneity of the field. In Figure. 4 we plot the convergence of the η-correlations to those expected from the Grand Canonical Ensemble (GCE), $\rho_{\mathrm{GCE}} \propto \exp(\mu_1\eta^+\eta^- + \mu_2 N_\uparrow + \mu_3 N_\downarrow)$, for 3 different choices of inhomogeneity. As expected the choice of $f(i)$ is arbitrary and, along with the choice of system parameters, only affects the transient dynamics and the rate of relaxation.

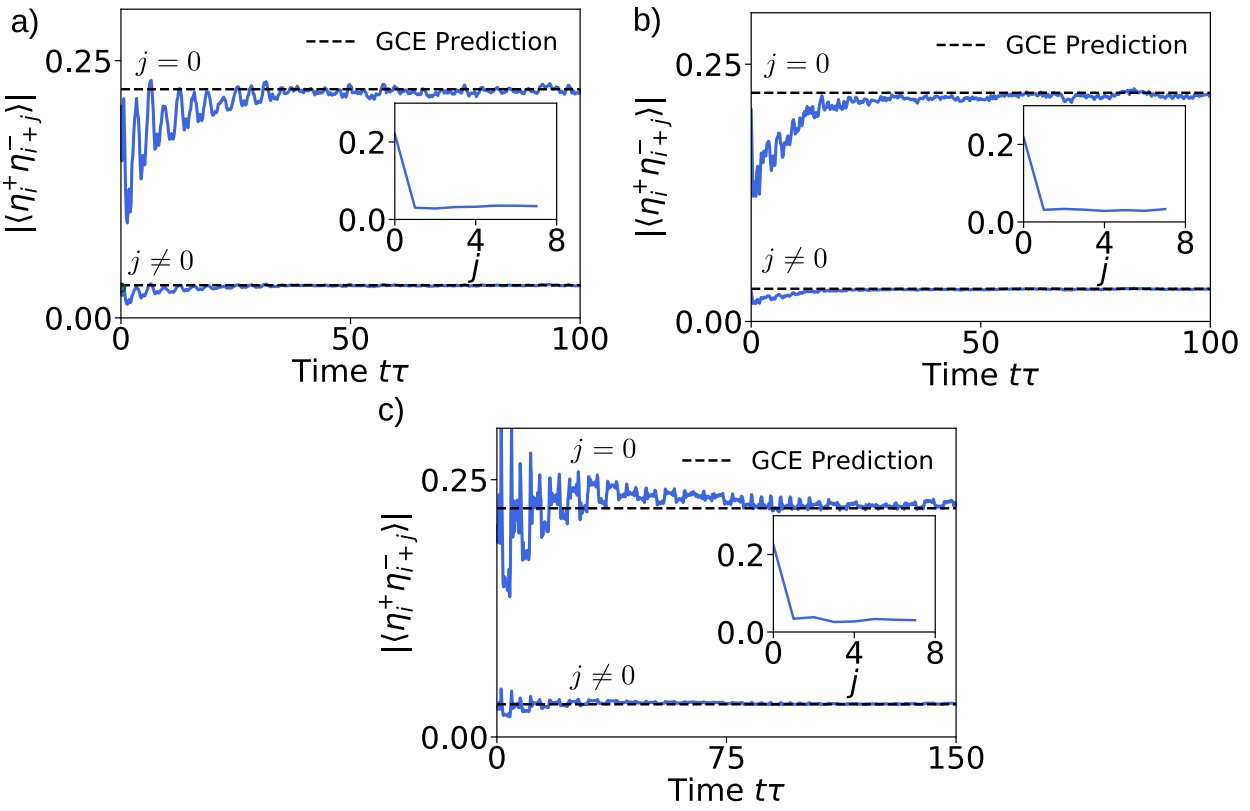

FIG. 4. Dynamics of the the η correlations $|\langle \eta_i^+ \eta_{i+j}^- \rangle|$ following a quench from the $U = \tau$ ground state of the $L = 8$ half-filled Hubbard model with $\langle S^z \rangle = 0$. The blue curves reflect the diagonal and off-diagonal correlations for a quench with the periodically driven Hamiltonian in Eq. (11) with $U = 6.0\tau$. The dashed lines indicate the prediction from the grand-canonical ensemble (GCE). (a) $V = 2.0U$, $\Omega = \tau$ and $f(i) = i$. (b) $V = 4.0U$, $\Omega = \tau$ and $f(i) = R[0, 2.0]$ where $R[0, 2.0]$ is a random number in the range 0.0 to 2.0. (c) $V = 6.0U$, $\Omega = \tau$ and $f(i) = (-1)^i$. Insets) The dependence of the correlations on distance, extracted for the curves at time $t\tau = 100.0$.

OSCILLATING COHERENCES

The Liouvillian in Eq. (1) also contains equally spaced imaginary eigenvalues [12] due to the existence of a ladder operator, $\eta^{\pm}$, of the Hamiltonian which also commutes with the Lindblad operators. The associated eigenvectors take the form of a raising of the steady state ρ_{ss}: $\rho_{nm} \propto (\eta^+)^n \rho_{ss} (\eta^-)^m$ with the eigenvalues $\lambda_{nm} = 2\mathrm{i}(m - n)\mu$. These states couple together sectors of the Hilbert Space with different particle numbers.

If one were able to initialise the system in a state with coherent superpositions between states with different particle numbers then, in the long-time limit, the dynamics of observables such as η^x should be oscillatory [12]. In the main text we have focused solely on the properties of the steady state by enforcing a specific number of particles within our simulations.

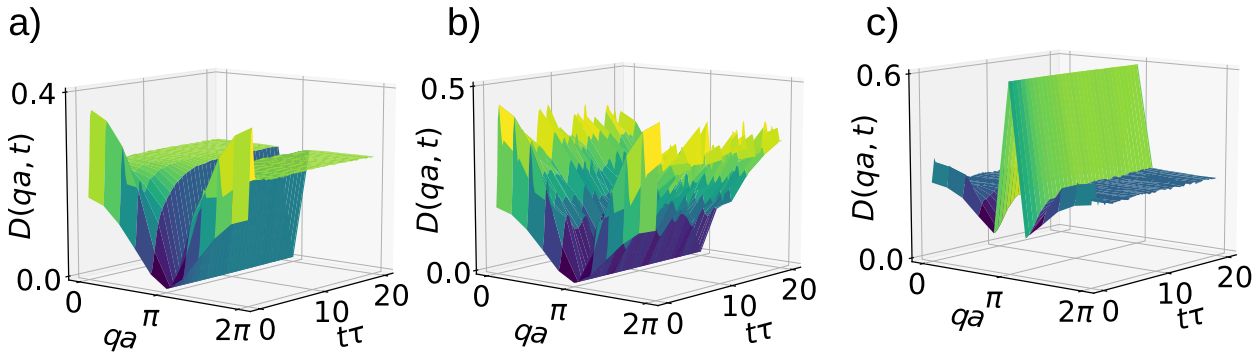

FIG. 5. Evolution of the structure factor $D(qa,t)$ in Eq. (12) over time for the 10 site Hubbard model at half-filling and $\langle S^z \rangle = 0$. The system is initialised in the ground state of H for $U = 4.0\tau$ and evolved under the same parameters but with a system-environment coupling of γ and an interaction strength of $U = \tau$. (a) $\gamma = 2.0\tau$. (b) $\gamma = 0.0$. (c) $\gamma = 2.0\tau$ and the system is initialised in the state $\propto (\eta^+)^2 |\psi\rangle$ where $|\psi\rangle$ is the ground state of the same Hamiltonian in a) and b) but with only 6 total particles.

QUASI-MOMENTUM DISTRIBUTIONS

We also plot the momentum distribution of the doublons following a quench from the ground state of the Hubbard model using the master equation (1). Figure 5. shows the evolution of the doublon structure factor

$$D(qa,t) = \frac{1}{L}\sum_{j,k=1}^{L} \langle c^\dagger_{\uparrow,j} c^\dagger_{\downarrow,j} c_{\downarrow,k} c_{\uparrow,k} e^{\mathrm{i}(k-j)qa} \rangle (t), \tag{12}$$

in time for the full range of quasi-momenta $q = 2\pi n/La \;\; n \in \{0, 1, ..., L-1\}$, with a the lattice spacing. In the long-time limit of the quench we see the flattening and equal excitation of all momenta modes, except for $qa = \pi$. This is characteristic of the steady states of the map in Eq. (1) due to their off-diagonal long-range order. The occupation of the momentum mode at $qa = \pi$ is equal to $\langle \eta^+ \eta^- \rangle / L$, it is a constant of the evolution and for states with increasing values of $\langle \eta^+ \eta^- \rangle$ the amplitude of this mode will grow (Fig. 5c), indicating the presence of a doublon condensate [13].

IMPLEMENTING SPIN DEPHASING IN A COLD ATOM SETUP

We now discuss the possibility of simulating the spin-dephased Hubbard model in a cold-atom setup. The Hamiltonian in Eq. 2 can be accurately realised by loading an ultracold gas of fermionic atoms into a lattice structure created with counter-propagating laser beams [8, 14, 15]. These optical lattices provide the experimentalist precise control over the microscopic parameters of the system.

In order to engineer dephasing solely in the spin degrees of freedom of the lattice we consider the

possibility of immersing the lattice into a homogeneous Bose-Einstein Consendate (BEC), which was also discussed in [12] in the context of achieving dephasing in the number basis of the Hubbard model. The interactions between the BEC and the lattice atoms create deformations in the condensate which can be described as polarons, or coherent states of phonons [16].

To explicitly derive the dynamics of the lattice in this environment we closely follow methodology of [16] and [17]. We start by writing the Hamiltonian $H_{\rm tot} = H_L + H_I + H_{\rm BEC}$ of the total system

$$\begin{aligned} H_L &= H, \\ H_I &= \int \big(\kappa_\uparrow \chi_\uparrow^\dagger(\mathbf{r})\chi_\uparrow(\mathbf{r})\phi^\dagger(\mathbf{r})\phi(\mathbf{r}) + \kappa_\downarrow \chi_\downarrow^\dagger(\mathbf{r})\chi_\downarrow(\mathbf{r})\phi^\dagger(\mathbf{r})\phi(\mathbf{r})\big)d\mathbf{r}, \\ H_{\rm BEC} &= \int \phi^\dagger(\mathbf{r})\bigg[-\frac{\nabla^2}{2m_b} + V_{\rm ext}(\mathbf{r}) + \frac{g}{2}\phi^\dagger(\mathbf{r})\phi(\mathbf{r})\bigg]\phi(\mathbf{r})d\mathbf{r}, \end{aligned} \tag{13}$$

with H_L, H_I and $H_{\rm BEC}$ being the lattice (see Eq. 2), interaction and BEC Hamiltonians respectively. The operators $\chi_\uparrow$ and $\chi_\downarrow$ are the field operators of the two fermionic levels which couple to the bosonic field ($\phi^\dagger(\mathbf{r})$) with amplitudes $\kappa_\uparrow$ and $\kappa_\downarrow$ respectively. The mass of a condensate atom is given by m_b, $V_{\rm ext}$ is an external trapping potential for the BEC and g is the interaction strength between the condensate atoms.

In order for the condensate to affect the dynamics of the lattice solely in the spin sector we set the coupling strengths to be equal and opposite, i.e. $\kappa_\uparrow = -\kappa_\downarrow = \kappa$. This could be achieved via Feshbach resonances [18, 19] which can be used to tune atomic scattering lengths over a wide range of values. It is also necessary that κ is sufficiently small $\kappa \ll gn^0\epsilon^D$, where n_0 is the BEC density in the centre of the trap, ϵ is the healing length and D is the system dimension [16]. By solving the Gross-Pitaevskii equation and treating the resulting deformations in the BEC as coherent states of phonons an effective, discretized, Hamiltonian for the system can be derived. We then trace out the phonon degrees of freedom, invoking the rotating wave and Born approximations, to derive a Master equation for the density matrix of the lattice $\rho_L(t)$

$$\begin{aligned} \partial_t \rho_L(t) = -i[H_g, \rho_L(t)] + \sum_{l,l'=1}^{M} f_{l,l'}(t)\big(s_l^z s_{l'}^z \rho_L(t) + \rho_L(t) s_l^z s_{l'}^z - 2 s_l^z \rho_L(t) s_{l'}^z\big), \\ H_g = H^{'} - \sum_{l,l'=1}^{M} g_{l,l'}(t) s_l^z s_{l'}^z, \end{aligned} \tag{14}$$

where $H^{'}$ is the Hubbard Hamiltonian (the parameters have been slightly modified due to the BEC presence) and $f_{l,l'}(t)$ and $g_{l,l'}(t)$ are a pair of time-dependent, short-range (based on 'typical' parameters for a BEC) functions which become time-independent in the long-time limit. Notably, however, the explicit form of these functions does not alter the strong symmetries of the system (they are still $\eta^+\eta^-$, S^z and $N_{\rm total}$). Therefore the steady states of this Master equation are guaranteed to have long-range η-paired correlations

in the long-time limit.

[1] A. J. Daley. Quantum trajectories and open many-body quantum systems. *Advances in Physics*, 63(2):77–149, Mar 2014.

[2] S. R. White. Density matrix formulation for quantum renormalization groups. *Phys. Rev. Lett.*, 69:2863–2866, Nov 1992.

[3] G. Vidal. Efficient classical simulation of slightly entangled quantum computations. *Phys. Rev. Lett.*, 91:147902, Oct 2003.

[4] S. Al-Assam, S. R. Clark, and D. Jaksch. The Tensor Network Theory library. *Journal of Statistical Mechanics: Theory and Experiment*, 2017(9):093102, 2017.

[5] A. Datta and G. Vidal. Role of entanglement and correlations in mixed-state quantum computation. *Phys. Rev. A*, 75:042310, Apr 2007.

[6] B. Buča and T. Prosen. A note on symmetry reductions of the Lindblad equation: transport in constrained open spin chains. *New Journal of Physics*, 14(7):073007, 2012.

[7] V. V. Albert, B. Bradlyn, M. Fraas, and L. Jiang. Geometry and response of Lindbladians. *Phys. Rev. X*, 6:041031, Nov 2016.

[8] M. Lewenstein, A. Sanpera, and V. Ahufinger. *Ultracold atoms in optical lattices : simulating quantum many-body systems*. Oxford University Press, Oxford, 2012.

[9] D. D. Awschalom, L. C. Bassett, A. S. Dzurak, E. L. Hu, and J. R. Petta. Quantum spintronics: Engineering and manipulating atom-like spins in semiconductors. *Science*, 339(6124):1174, Mar 2013.

[10] Marko Žnidarič. Relaxation times of dissipative many-body quantum systems. *Phys. Rev. E*, 92:042143, Oct 2015.

[11] T. Can. Random Lindblad dynamics. *arXiv:1902.01442*, 2019

[12] B. Buca, J. Tindall, and D. Jaksch. Non-stationary coherent quantum many-body dynamics through dissipation. *Nature Communications*, 10(1):1730, 2019.

[13] O. Penrose and L. Onsager. Bose-Einstein condensation and liquid helium. *Phys. Rev.*, 104:576–584, Nov 1956.

[14] D. Jaksch and P. Zoller. The cold atom Hubbard toolbox. *Annals of Physics*, 315(1):52–79, 2005.

[15] M. Lewenstein, A. Sanpera, V. Ahufinger, B. Damski, A. Sen De, and U. Sen. Ultracold atomic gases in optical lattices: mimicking condensed matter physics and beyond. *Advances in Physics*, 56(2):243–379, Mar 2007.

[16] A. Klein, M. Bruderer, S. R. Clark, and D. Jaksch. Dynamics, dephasing and clustering of impurity atoms in Bose-Einstein condensates. *New Journal of Physics*, 9(11):411–411, 2007.

[17] M. Bruderer, A. Klein, S. R. Clark, and D. Jaksch. Polaron physics in optical lattices. *Phys. Rev. A*, 76:011605, Jul 2007.

[18] M. Theis, G. Thalhammer, K. Winkler, M. Hellwig, G. Ruff, R. Grimm, and J. Hecker Denschlag. Tuning the scattering length with an optically induced Feshbach resonance. *Phys. Rev. Lett.*, 93:123001, Sep 2004.

[19] S. Inouye, M. R. Andrews, J. Stenger, H.-J. Miesner, D. M. Stamper-Kurn, and W. Ketterle. Observation of Feshbach resonances in a Bose-Einstein condensate. *Nature*, 392(6672):151–154, 1998.